Conduction subbands in a GaAs/$Al_xGa_{1-x}As$ quantum well: Comparing different k·p models

Paul von Allmen*
IBM Research Division, Zurich Research Laboratory, 8803 Rüschlikon, Switzerland
(Received 3 January 1992)

The energy dispersion of the conduction subbands in a GaAs/$Al_xGa_{1-x}As$ superlattice is calculated by using a **k·p** Hamiltonian that includes different number of bands. The most accurate model includes the Γ_6^c, Γ_7^v, Γ_8^v, Γ_7^c, and Γ_8^c bands. The resulting subband dispersion is compared with that obtained when the coupling of the Γ_6^c band with the Γ_7^v and Γ_8^v and/or Γ_7^c and Γ_8^c bands is neglected. We also consider the 2×2 **k·p** Hamiltonian with terms up to the order k^4. The subband dispersions are analyzed quantitatively by fitting the numerical result to the analytical expression obtained with the invariant expansion technique. The subbands are found to be significantly different with the various models. The differences are ascribed to the different bulk band dispersions obtained with different **k·p** Hamiltonians and to the variation of the band parameters in the well and barrier materials.

Many authors have calculated the dispersion of the conduction subbands in multiple-quantum-well structures. In the simplest model, the Schrödinger equation is solved for one particle of mass m in a square well. Later works show the importance of the difference between the effective masses in the well and in the barrier for the determination of the energy levels.[1] The effect of the nonparabolicity of the bulk conduction band was taken into account with various levels of sophistication. Reference 1 uses an energy-dependent effective mass obtained by projecting the **k·p** Hamiltonian resulting from the coupling with the light hole and the split-off bands on the conduction-band subspace. Second-order terms in k were neglected in this procedure. Coupling with the light hole and the split-off bands was fully included in Refs. 2 and 3. Reference 4 takes into account the nonparabolicity of the bulk conduction band by using the energy dispersion relation that includes terms up to the order k^4, but the spin-splitting term was neglected. A similar procedure was followed in Ref. 5, where the bulk 2×2 **k·p** Hamiltonian is used for the Γ_6^c conduction-band subspace with terms up to k^4. In this way the spin splitting is also obtained.

For bulk GaAs it was shown in Ref. 6 that the coupling of the Γ_6^c conduction band, not only with the Γ_7^v and Γ_8^v valence bands but also with the Γ_7^c and Γ_8^c conduction bands, is important to describe its nonparabolicity and warping accurately. This leads to a 14×14 **k·p** Hamiltonian. The aim of this paper is to present the subband energy dispersion for a quantum well obtained with a 14×14 Hamiltonian and to compare it to the results obtained when fewer bands are included. I shall also consider the case of the 2×2 Hamiltonian with terms up to k^4 as in Ref. 5.

The results obtained here are of significance, e.g., for the evaluation of the width of the intersubband absorption line. It was shown that for this purpose the effective masses of the subbands involved have to be known accurately.[7]

Let us consider a GaAs/$Al_{0.35}Ga_{0.65}As$ superlattice with $L_w=80$ Å and $L_b=250$ Å for the widths of the wells and the barriers, respectively. The effective-mass equation to be solved was derived in Ref. 8 and is written as follows:

$$\sum_{n'}^{N}\left[\delta_{nn'}\left[E_{n'}(z)+\frac{\hbar^2k_{\parallel}^2}{2m_0}-\frac{\hbar^2\partial_{zz}^2}{2m_0}-E\right]+\mathbf{P}_{nn'}(z)\left[\mathbf{k}_{\parallel}+\mathbf{e}_z\frac{\partial_z}{i}\right]+\sum_{\alpha,\beta}\Gamma_{nn'}^{\alpha\beta}(z)\left[\mathbf{k}_{\parallel}+\mathbf{e}_z\frac{\partial_z}{i}\right]_{\alpha}\times\left[\mathbf{k}_{\parallel}+\mathbf{e}_z\frac{\partial_z}{i}\right]_{\beta}\right]\varphi_{n'}(z)=0\ , \quad (1)$$

where $E_n(z)$ are the band-edge energies of the N bands considered. When z is in the well (barrier) the values to be taken are those for GaAs ($Al_{0.35}Ga_{0.65}As$). At the interface the variation is assumed to be abrupt. The momentum matrix elements $\mathbf{P}_{nn'}(z)$ and the renormalization constants $\Gamma_{nn'}^{\alpha\beta}(z)$ are defined in a similar way. The momentum parallel to the layers is $\mathbf{k}_{\parallel}$; $\mathbf{e}_z$ is the unit vector in direction z (perpendicular to the layers), and m_0 is the mass of the free electron.

As is well known from Ref. 9, the matrix of differential operators acting on the envelope functions $\varphi_n(z)$ in the effective-mass equation is the bulk **k·p** Hamiltonian with ∂_z/i replacing k_z. The operator acting on φ_n as it is written in (1) is not Hermitian. It can be made so by symmetrizing the terms containing derivatives and space-varying coefficients. For the term with $\mathbf{P}_{nn'}(z)$ it can be shown that the terms to be added for symmetrization are of the same order of magnitude as those neglected when deriving the effective-mass equation.[8] For the term with $\Gamma_{nN}^{\alpha\beta}(z)$, Ref. 10 shows that the Hermitian form is readily obtained when applying the Löwdin renormalization procedure.

Here I use the bulk **k·p** Hamiltonian of Ref. 6 and include the coupling term Δ^- between the Γ_{15}^v and Γ_{15}^c bands, originating from the spin-orbit coupling potential in the crystal Hamiltonian.[11] The notation for the band-edge energies and for the momentum matrix elements is

given in Fig. 1.

The numerical values for the momentum matrix elements P and P' are obtained from the effective mass m_c^* and Landé factor g_c^* at Γ_6^c:[12]

$$\frac{m_0}{m_c^*}-1=\frac{2m_0}{3\hbar^2}\left[\frac{2P_2^2}{E_0}+\frac{P_1^2}{E_0+\Delta_0}\right]-\frac{2m_0}{3\hbar^2}\left[\frac{2P_2'^2}{E_0'+\Delta_0'-E_0}+\frac{P_1'^2}{E_0'-E_0}\right]+\frac{2m_0}{\hbar^2}A'^{(14B)}, \tag{2}$$

$$\frac{g_c^*}{g_0}-1=\frac{2m_0}{3\hbar^2}\left[\frac{P_1^2}{E_0+\Delta_0}-\frac{P_2^2}{E_0}\right]+\frac{2m_0}{3\hbar^2}\left[\frac{P_2'^2}{E_0'+\Delta_0'-E_0}-\frac{P_1'^2}{E_0'-E_0}\right]+C'^{(14B)}, \tag{3}$$

with

$$P_2=P-\eta_2P',\quad P_1=P+\eta_1P',\qquad P_2'=P'+\eta_2P,\quad P_1'=P'-\eta_1P, \tag{4}$$

where

$$\eta_1=\frac{2\Delta^-}{3(E_0'+\Delta_0)},\quad \eta_2=\frac{\Delta^-}{3(E_0'+\Delta_0')}. \tag{5}$$

Expressions (2) and (3) are identical to those found in Ref. 12 if η_1 and η_2 are zero. As seen from (5), the terms with η_1 and η_2 come from the k-independent coupling of the Γ_{15}^c with the Γ_{15}^v bands.

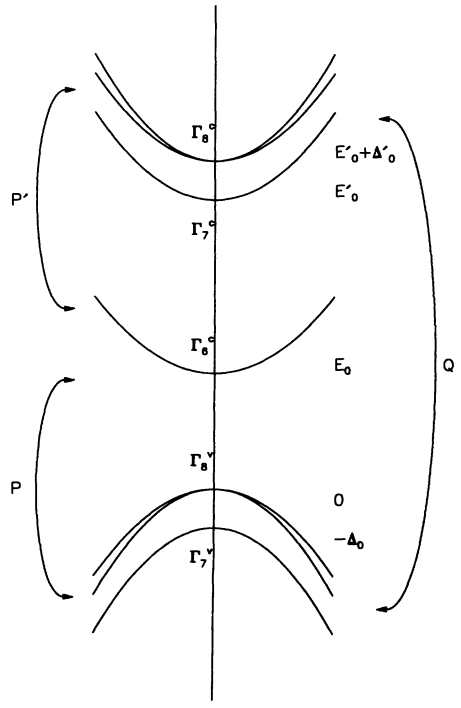

FIG. 1. Schematic band structure near $k=0$ for GaAs and $Al_xGa_{1-x}As$.

The renormalization constants have different values depending on the number of bands N considered. Their explicit expressions can be found in Table I. The Luttinger parameters $\gamma_\nu^{(6B)}$ ($\nu=1,\ldots,3$) given in the literature are defined for a 6-band model where the coupling of the valence with the conduction bands is neglected. The renormalization constant in the diagonal terms of the 2×2 block for the Γ_6^c subspace is A', and B is the renormalization constant appearing in the blocks coupling the Γ_6^c to the Γ_8^v and Γ_7^v bands.[13] The latter constant is responsible for the spin splitting in the 8-band model where the coupling with the Γ_7^c and Γ_8^c bands is neglected.

The numerical values of all the band parameters at $T=4.2$ K for the well and the barrier bulk materials are given in Table II together with the references from which they were taken. For $Al_{0.35}Ga_{0.65}As$ the following band parameters are obtained from a linear interpolation between the values for GaAs and AlAs: Δ_0, E_0', Δ_0', g_c^*, γ_1, γ_2, and γ_3. When no data for AlAs are available in the literature (for Δ^-, Q, and $A'^{(14B)}$), we take the same values as for GaAs. For the evaluation of P and P' from (2) and (3), we use $C'^{(14B)}=0.02$ for both GaAs and $Al_{0.35}Ga_{0.65}As$.[12] As mentioned in the Introduction, we also need the bulk 2×2 $\mathbf{k}\cdot\mathbf{p}$ Hamiltonian for the Γ_6^c subspace with terms up to the order k^4. It has been derived, e.g., in Ref. 5, and is given by the following expression:

$$H^{(4)}(\mathbf{k})=\left\{\frac{\hbar^2k^2}{2m_c^*}+\alpha k^4+\beta(k_y^2k_z^2+k_z^2k_x^2+k_x^2k_y^2)\right\}1+\gamma\{\sigma_xk_x(k_y^2-k_z^2)+\sigma_yk_y(k_z^2-k_x^2)+\sigma_zk_z(k_x^2-k_y^2)\}, \tag{6}$$

where 1 is the 2×2 unit matrix and σ_x, σ_y, and σ_z are the Pauli matrices.

Diagonalizing (6) and fitting the resulting expressions

TABLE I. Renormalization constants for the various $\mathbf{k}\cdot\mathbf{p}$ models considered.

$$\Lambda=\frac{4m_0}{9\hbar^2}[2P_2^2/E_0+P_1^2/(E_0+\Delta_0)],$$

$$\Lambda'=\frac{4m_0Q^2}{9\hbar^2}[1/(E_0'+\Delta_0/2)+2/(E_0'+\Delta_0'+(\Delta_0/2)],$$

$$M=-\tfrac{1}{3}[2P_2'^2/(E_0'+\Delta_0'-E_0)+P_1'^2/(E_0'-E_0)],$$

$$M'=\tfrac{1}{3}[2P_2^2/E_0+P_1^2/(E_0+\Delta_0)],$$

$$B=\frac{2Q}{3}[2P_2'/(E_0'+\Delta_0'-E_0)+P_1'/(E_0'-E_0)].$$

	6 bands (Γ_7^v,Γ_8^v)	8 bands ($\Gamma_7^v,\Gamma_8^v,\Gamma_6^c$)	14 bands ($\Gamma_7^v,\Gamma_8^v,\Gamma_6^c,\Gamma_7^c,\Gamma_8^c$)
γ_1	$\gamma_1^{(6B)}$	$\gamma_1^{(6B)}-\frac{\Lambda}{2}$	$\gamma_1^{(6B)}-\frac{\Lambda}{2}-\Lambda'$
γ_2	$\gamma_2^{(6B)}$	$\gamma_2^{(6B)}-\frac{\Lambda}{4}$	$\gamma_2^{(6B)}-\frac{\Lambda}{4}+\frac{\Lambda'}{4}$
γ_3	$\gamma_3^{(6B)}$	$\gamma_3^{(6B)}-\frac{\Lambda}{4}$	$\gamma_3^{(6B)}-\frac{\Lambda}{4}-\frac{\Lambda'}{4}$
A'	$A'^{(14b)}+M+M'$	$A'^{(14B)}+M$	$A'^{(14B)}$
B	—	B	0

TABLE II. Band parameters for GaAs and $Al_{0.35}Ga_{0.65}As$ at $T=4.2$ K.

	14 bands		8 bands		6 bands	
	GaAs	$Al_xGa_{1-x}As$	GaAs	$Al_xGa_{1-x}As$	GaAs	$Al_xGa_{1-x}As$
γ_1	−0.58	0.16	0.91	1.64	6.85[b]	5.59[b]
γ_2	−0.50	−0.02	−0.87	−0.39	2.10[b]	1.59[b]
γ_3	−0.44	−0.04	−0.07	0.33	2.90[b]	2.31[b]
A' (eV Å^2)	−6.477[a]	−6.477[a]	−10.168	−6.994	53.570	36.106
B (eV Å^2)	0	0	13.79	5.56	0	0
E_0 (eV)	1.519[b]	1.972[c]				
Δ_0 (eV)	0.341[b]	0.317[b]				
E_0' (eV)	4.488[b]	4.527[b]				
Δ_0' (eV)	0.171[b]	0.171[b]				
Δ^- (eV)	−0.085[c]	−0.085[c]				
m_c^* (m_0)	0.0664[b]	0.0955[e]				
g_c^*	−0.44[b]	0.81[b]				
P (eV Å)	10.16	9.44				
P' (eV Å)	3.37	1.17				
Q (eV Å)	6.26[d]	6.26[d]				

[a]Reference 12.
[b]Reference 15.
[c]Reference 11.
[d]Reference 17.
[e]Reference 16.

for the eigenvalues to the energy dispersion obtained by diagonalizing numerically the 14×14 $\mathbf{k}\cdot\mathbf{p}$ Hamiltonian yields the coefficients m_c^*, α, β, and γ. Table III presents these coefficients for GaAs and $Al_{0.35}Ga_{0.65}As$ at $T=4.2$ K. The values obtained for GaAs are close to those found in Ref. 6. Expression (6) with the values in Table III reproduces the numerical energy dispersion up to $k=0.05$ Å^{-1} with a maximum deviation of 0.5 meV.

With (6) we can write an effective-mass equation very similar to (1):

$$\sum_{n'=1}^{2} \mathbf{H}_{nn'}^{(4)}\left[z;\mathbf{k}_{\parallel},\frac{\partial_z}{i}\right]\varphi_{n'}(z)=E\varphi_n(z)\ , \tag{7}$$

where the z dependence in $H^{(4)}$ indicates that the band parameters m_c^*, α, β, and γ are those of GaAs ($Al_{0.35}Ga_{0.65}As$) for z in the well (barrier). As for (1) the operator on φ_n can be made Hermitian by symmetrizing the terms with derivatives and space-varying coefficients.

The effective-mass equation [(1) or (7)] is solved by expanding the envelope functions and the space-varying band parameters on a plane-wave basis. It was found that for the structure considered here the convergence on the eigenvalues is achieved with 21 plane waves with a maximum estimated error of 0.5 meV.

Figure 2(a) shows the energy dispersion of the average

TABLE III. Energy dispersion parameters for the conduction band for GaAs and $Al_{0.35}Ga_{0.65}As$ at $T=4.2$ K.

	GaAs	$Al_{0.35}Ga_{0.65}As$
m_c^* (m_0)	0.0669	0.0958
α (eV Å^4)	−1585	−748
β (eV Å^4)	−1445	−985
γ (eV Å^3)	18.3	7.6

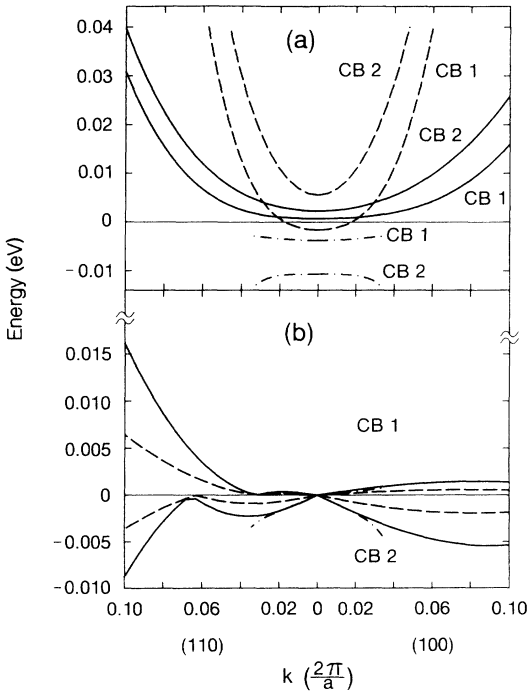

FIG. 2. (a) Difference between the subband energy dispersion averaged over the two spins obtained with the 14B model and that obtained with the 8B model (solid line), the 6B model (dashed line), and the $6C(k^4)$ model (dash-dotted line). (b) Spin splitting of the first and second conduction subband in the upper and lower half-plane, respectively, solid line, 14B model; dashed line, 8B model; and dash-dotted line, $6B(k^4)$ model. The structure is a $GaAs/Al_{0.35}Ga_{0.65}As$ superlattice at $T=4.2$ K, $L_w=80$ Å and $L_b=250$ Å are the widths of the wells and the barriers, respectively.

over the two spin bands and Fig. 2(b) gives the spin splitting. For a more quantitative overview of the results the subband energy dispersion was fitted to the analytical expression obtained with the invariant expansion technique (see, e.g., Ref. 5).

The symmetry group for the superlattice is D_{2d}. The corresponding combinations of the momentum $\mathbf{k}$ with the irreducible representations to which they belong are listed in Table IV. The set of basis matrices in the two-dimensional subspace associated with each subband includes the 2×2 unit matrix (belonging to Γ_1) and the Pauli matrices (belonging to Γ_5). The 2×2 $\mathbf{k}\cdot\mathbf{p}$ Hamiltonian for the subband number j is obtained from the multiplication tables for the irreducible representations of the group D_{2d}:[14]

$$H_j^{(4)}(\mathbf{k}_\parallel)=\left[E_{0j}+\frac{\hbar^2k_\parallel^2}{2m_j^*}+\alpha_jk_\parallel^4+\beta_jk_x^2k_y^2\right]1 +\Omega_x\sigma_x+\Omega_y\sigma_y\ , \tag{8}$$

with

$$\Omega_x=\gamma_1^{(j)}k_x+\gamma_2^{(j)}k_xk_y^2+\gamma_3^{(j)}k_\parallel^2k_x\ , \qquad \Omega_y=\gamma_1^{(j)}k_y+\gamma_2^{(j)}k_x^2k_y+\gamma_3^{(j)}k_\parallel^2k_y\ . \tag{9}$$

The eigenvalues of $H_j^{(4)}$ are given by the following expression:

$$E_j(\mathbf{k}_\parallel)=E_0^{(j)}+\frac{\hbar^2k_\parallel^2}{2m_j^*}+\alpha_jk_\parallel^4+\beta_jk_x^2k_y^2 \pm|\gamma_1^{(j)}(k_x-ik_y)-i\gamma_2^{(j)}k_xk_y(k_x+ik_y) +\gamma_3^{(j)}k_\parallel^2(k_x-ik_y)|\ . \tag{10}$$

This expression is fitted to the subbands obtained by solving the effective-mass equation. The resulting subband parameters $E_0^{(j)}$, m_j^*, α_j, β_j, and $\gamma_\nu^{(j)}$ ($\nu=1,\ldots,3$) are presented in Table V.

Figure 2(a) shows the difference between the subband dispersion averaged over the two spins for all the models considered and that for the 14-band (14B) model. In the 6-band (6B) model, the Γ_6^c conduction band is uncoupled from all the other bands. We see that the curvature of the two subbands is larger than in the 14B model. The reason for this is that the nonparabolicity of the conduction band has been neglected. The effective mass in the first subband is smaller than that in the second one because the first state is better confined within the well material which has a smaller effective mass. Table V shows that warping and spin splitting are absent as expected since these properties are strictly associated with the coupling of the Γ_6^c with other bands. The subbands are slightly nonparabolic, which is an effect of the confining potential.

TABLE IV. Combinations of the momentum $\mathbf{k}$ and the irreducible representations to which they belong for the D_{2d} symmetry group.

Γ_1:	$1, k_\parallel^2, k_\parallel^4, k_x^2k_y^2$
Γ_4:	k_xk_y
Γ_5:	$(k_x,k_y); k_\parallel^2(k_x,k_y); k_xk_y(k_y,k_x)$

In the 8-band (8B) model, the Γ_6^c conduction band is coupled with the Γ_7^v and Γ_8^v valence bands. From Fig. 2 and Table V we see that the energy at $k=0$, the effective mass, the nonparabolicity, the warping, and the spin splitting for the two subbands are smaller than in the 14B model. This is a direct consequence of the smaller nonparabolicity, warping, and spin splitting in the bulk conduction band for the 8B model.[6] The effective masses are larger than in the 6B model because the bulk conduction band is nonparabolic.

In the 6B model with terms of the order up to k^4 [6$B(k^4)$], the curves in Fig. 2 are shown only up to about $k=0.04$ Å^{-1} because the band parameters of Table IV were obtained by fitting the numerical curves up to only $k=0.05$ Å^{-1}. We see that the effective masses are slightly smaller and that the nonparabolicity and warping are larger than in the 14B model; the spin splitting is almost the same, while the energies at $k=0$ are significantly smaller. It is interesting to note that the origin of these differences is not that the bulk $\mathbf{k}\cdot\mathbf{p}$ Hamiltonian gives a different dispersion in the 6$B(k^4)$ model than in the 14B model. The differences come from the way the coupling

TABLE V. Energy dispersion parameters for the two conduction subbands in a $GaAs/Al_{0.35}Ga_{0.65}As$ superlattice at $T=4.2$ K; $L_w=80$ Å and $L_b=250$ Å are the widths of the wells and the barriers, respectively.

		E_0 (meV)	m^* (m_0)	α (eV Å^4)	β (eV Å^4)	γ_1 (eV Å)	γ_2 (eV Å^3)	γ_3 (eV Å^3)
14B	$CB1$	45.8	0.0722	−1344	−1340	0.026	−36.3	−1.63
	$CB2$	166.6	0.0874	−853	−1144	0.086	−27.0	−3.84
8B	$CB1$	46.5	0.0715	−1278	−855	0.011	−17.3	−0.88
	$CB2$	168.9	0.0844	−828	−706	0.036	−11.4	−2.21
6B	$CB1$	44.2	0.0674	−29	0	0	0	0
	$CB2$	172.2	0.0708	−148	0	0	0	0
6$B(k^4)$	$CB1$	42.0	0.0709	−1601	−1419	0.018	−35.8	0.084
	$CB2$	156.0	0.0872	−2028	−1357	0.082	−33.7	11.78

between the bands and the solution of the effective-mass equation are related. In the $14B$ model they are on the same footing: both are included in a single step that is the diagonalization of the matrix corresponding to the effective-mass equation. In the $6B(k^4)$ model the coupling between the bands is first renormalized and represented by the band parameters m^*, α, β, and γ. The differential equations are solved in a second step.

For the three models compared to the $14B$ model we obtained the general result that the difference is larger for the second subband. This is expected since the second subband state corresponds to a larger k_z in the bulk band dispersion for which the differences between the models is larger.

In conclusion, it has been shown that the inclusion of different number of bands in the effective-mass equation significantly changes the subband energy dispersion in a superlattice. I demonstrated that two distinct mechanisms are responsible for these changes. First, the subband dispersion is different for two models if the corresponding $\mathbf{k}\cdot\mathbf{p}$ Hamiltonian yields different bulk band dispersions. Second, I have shown that it is important to treat the coupling between the bands and the solution of the differential equations in the effective-mass equation on equal footing in order to obtain accurate results.

I would like to thank M.-A. Dupertuis, A. Pasquarello, C. Andreani, and G. Bastard for useful discussions.

---

*Present address: Beckman Institute, University of Illinois at Urbana-Champaign, Urbana, IL 61801.

[1]G. Bastard, Phys. Rev. B **24**, 5693 (1981).
[2]M. F. H. Schuurmans and G. W. 't Hooft, Phys. Rev. B **31**, 8041 (1985).
[3]R. Eppenga, M. F. H. Schuurmans, and S. Colak, Phys. Rev. B **36**, 1554 (1987).
[4]U. Eckenberg (private communication).
[5]F. Malcher, G. Lommer, and U. Rössler, Superlatt. Microstruct. **2**, 267 (1986).
[6]U. Rössler, Solid State Commun. **49**, 943 (1984).
[7]P. von Allmen, M. Berz, F.-K. Reinhart, and G. Harbeke, Superlatt. Microstruct. **5**, 259 (1989).
[8]P. von Allmen, preceding paper, Phys. Rev. B **46**, 15 376, (1992).
[9]J. M. Luttinger, Phys. Rev. **102**, 1030 (1956).
[10]M. G. Burt, Semicond. Sci. Technol. **3**, 739 (1988).
[11]M. Cardona, N. E. Christensen, and G. Fasol, Phys. Rev. B **38**, 1806 (1988).
[12]C. Hermann and C. Weisbuch, Phys. Rev. B **15**, 823 (1977).
[13]H.-R. Trebin, U. Rössler, and R. Ranvaud, Phys. Rev. B **20**, 686 (1979).
[14]G. F. Koster, J. O. Dimmock, R. G. Wheeler, and H. Statz, *Properties of Thirty Two Point Groups* (MIT Press, Cambridge, MA, 1963).
[15]*Landolt-Börnstein Tables,* edited by O. Madelung, M. Shultz, and H. Weiss (Springer, Berlin, 1987).
[16]H. J. Lee, L. Y. Juravel, J. C. Woolley, and A. J. Spring Thorpe, Phys. Rev. B **21**, 659 (1980).
[17]W. Zawadsky, P. Pfeffer, and H. Sigg, Solid State Commun. **53**, 777 (1985).